Filamentary structure of streamers in Transient Luminous Events

Paweł Jujeczko

Seminarium Zakładu Równań Fizyki Matematycznej

29.02.2024

MIM UW

Transient Luminous Events (TLE)

- Occur over big thunderstorms, last from 1ms (ELVES) to hundreds ms (sprite, jet)
- Sprites, alt. 40-80km (Franz et al., 1990)

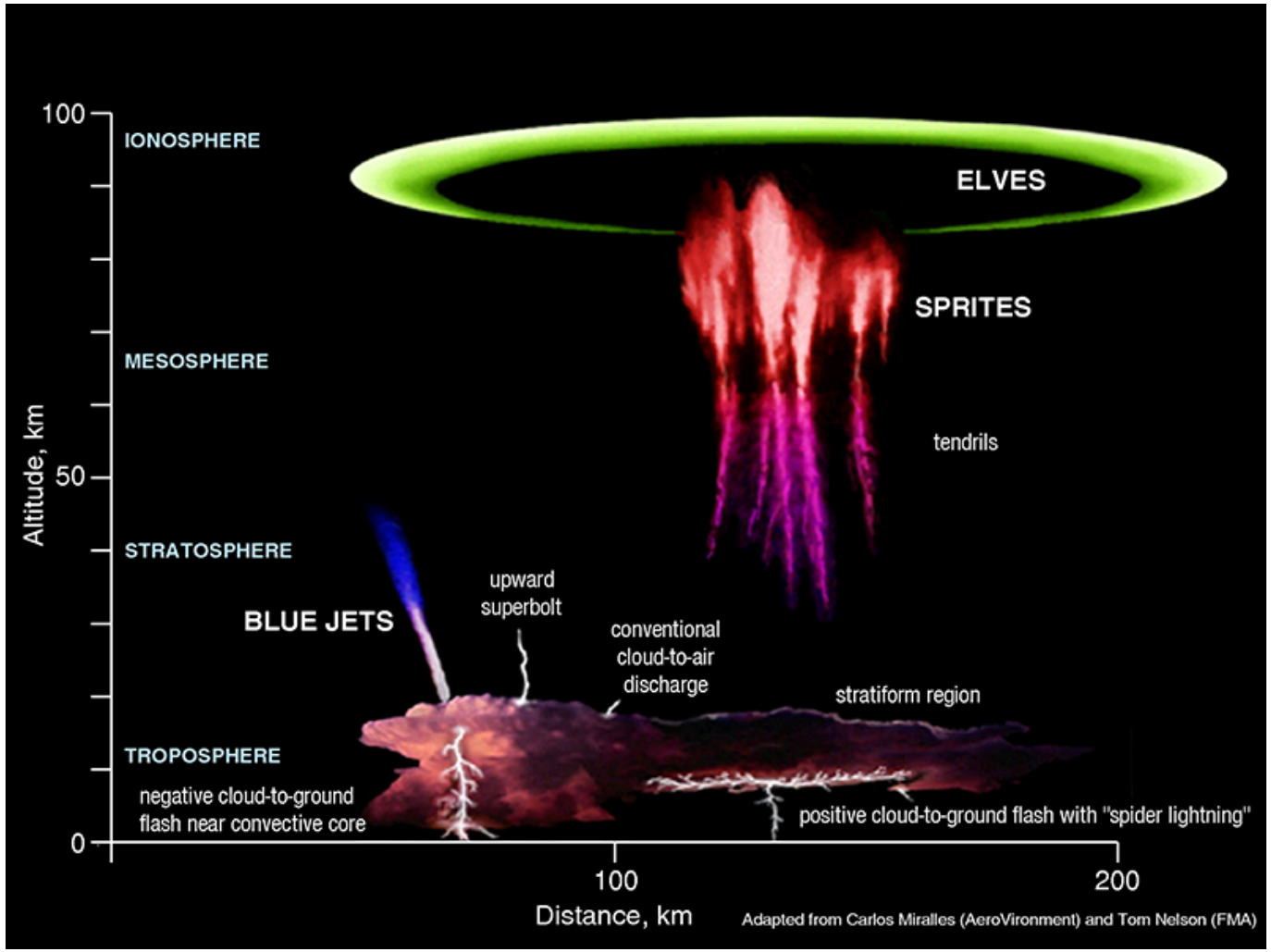

Sprites over a thundercloud

Astronomy Picture of the Day

Discover the cosmos! Each day a different image or photograph of our fascinating universe is featured, along with a brief explanation written by a professional astronomer.

2021 January 4

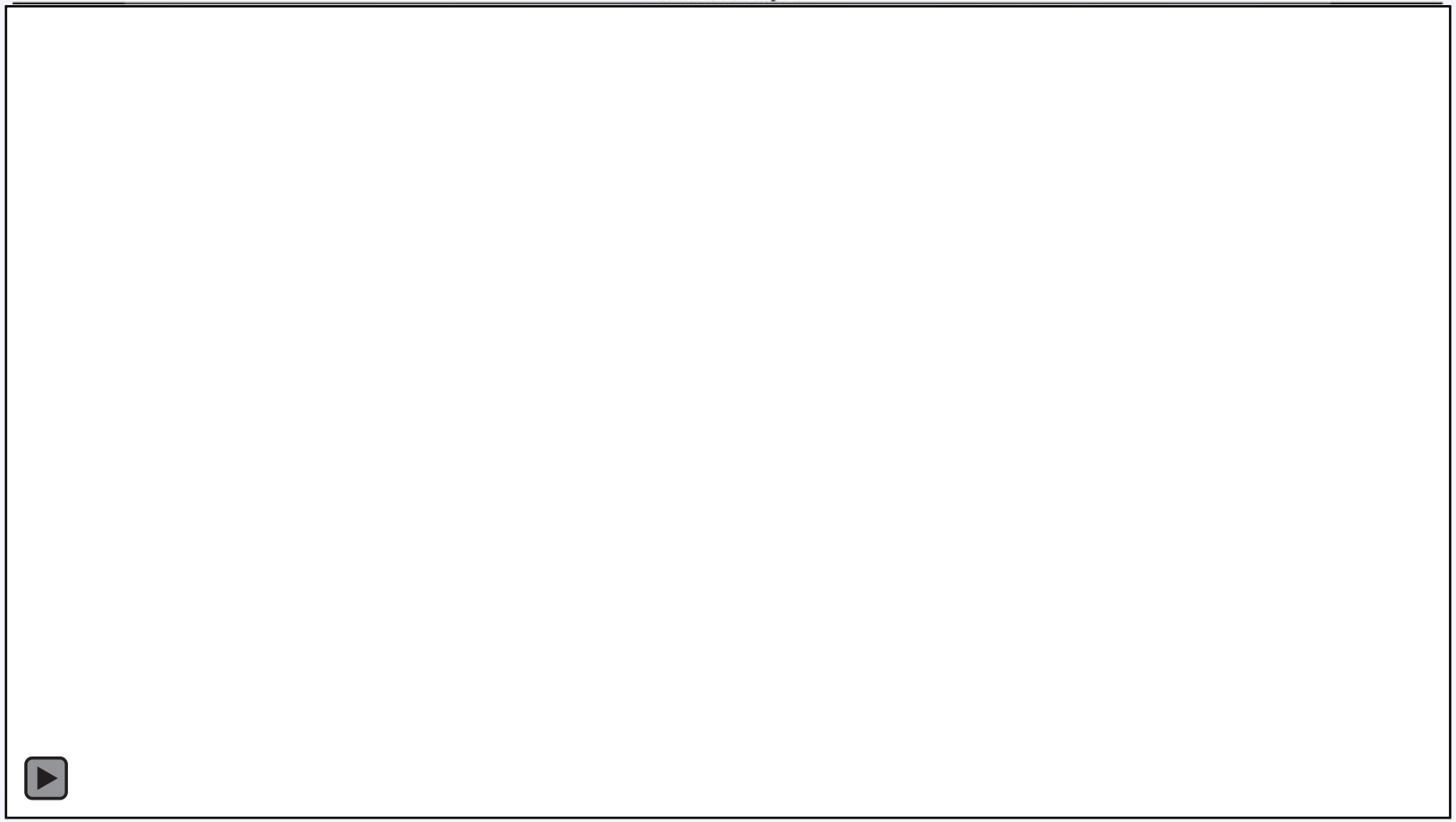

Sprite Lightning at 100,000 Frames Per Second
Video Credit & Copyright: Matthew G McHarg, Jacob L Harley, Thomas Ashcraft, Hans Nielsen

xplanation: What causes sprite lightning? Mysterious bursts of light in the sky that momentarily resemble gigantic jellyfish have been recorded for over 30 years, but apart from a general association with positive cloud-to-ground ghtning, their root cause remains unknown. Some thunderstorms have them -- most don't. Recently, however, high speed videos are better detailing how sprites actually develop. The featured video, captured in mid-2019, is fast hough -- at about 100,000 frames per second -- to time-resolve several sprite "bombs" dropping and developing into the multi-pronged streamers that appear on still images. Unfortunately, the visual clues provided by videos like ese do not fully resolve the sprite origins mystery. High speed vidoes do indicate to some researchers, though, that sprites are more likely to occur when plasma irregularities exist in the upper atmosphere.

Filamentary structure of sprites

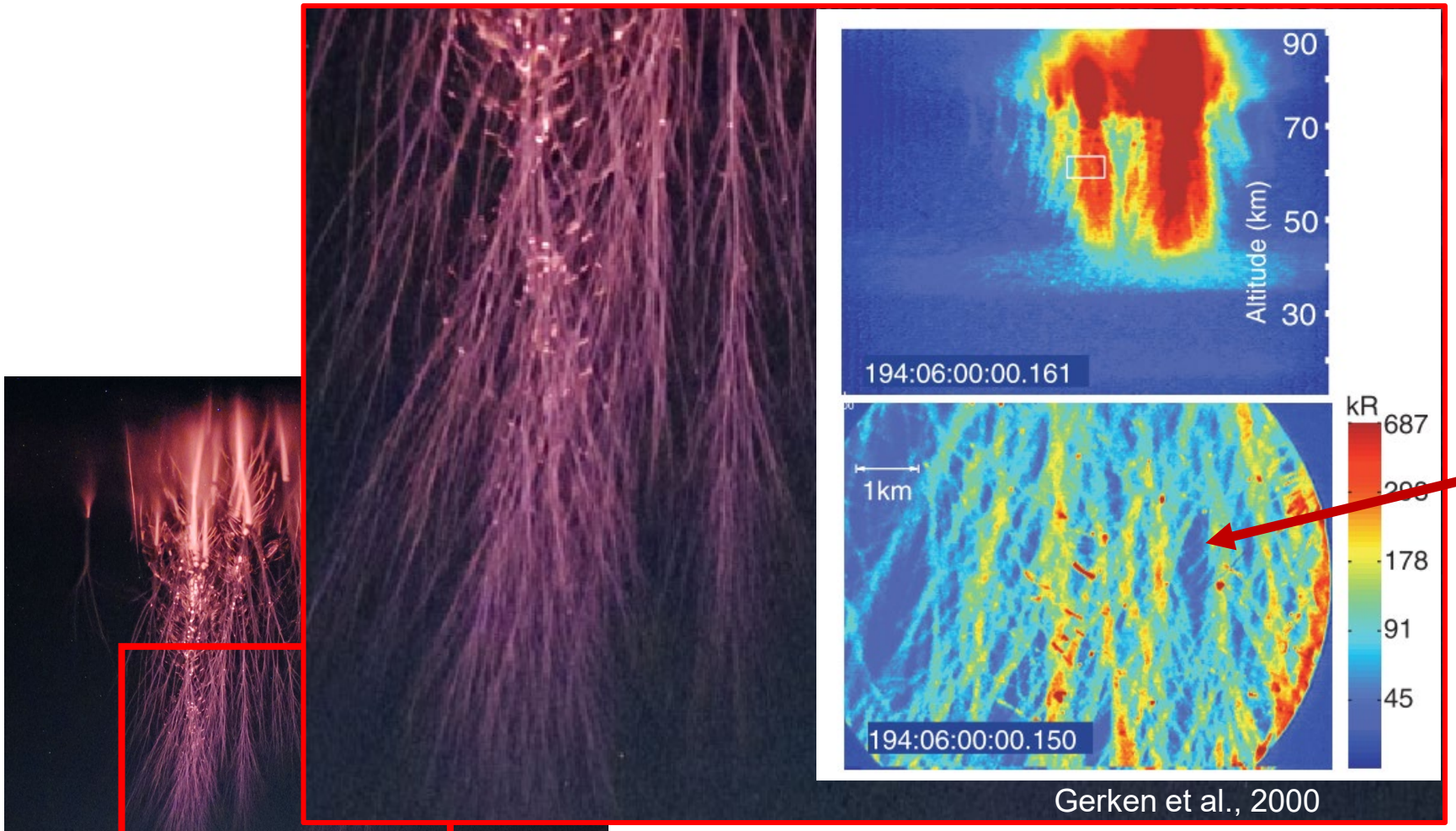

These are streamer channels
Why do they split/branch?

What is a streamer?

- Electric discharge in gas (St Elmo's fires, plasma balls)
- Streamer's head is an expanding structure that ionizes the gas in the front, ($E_h > E_0$); behind lays a weakly-ionized plasma channel ($E_s \ll E_h$)

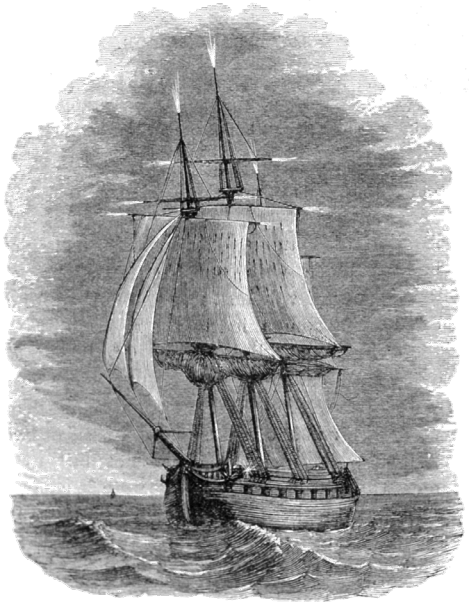

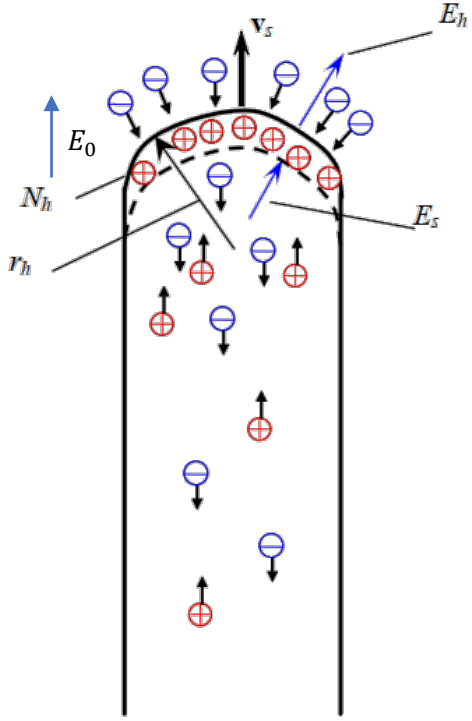

Fig. 2. A positive streamer model. Here v_s is streamer velocity, r_h is curvature radius of the streamer head, N_h is number density of uncompensated/unbalanced positive charges, E_h is electric field in front of the streamer head, and E_s is electric field inside the streamer.

Surkov & Hayakawa, 2012

Problems in modeling TLE streamers

- In-situ measurements not available in the mesosphere (only brief rocket soundings and indirect measurement) and inside TLE streamers (indirect measurements, scaling laws)
- **At first TLE streamer plasma properties were to be estimated**
- Choosing the modeling method (*e.g. Adams-Bashforth, Particle-in-Cell)*; Trade-offs: precision vs computation time and code complication; Choosing plasma theory to work in (kinetic, fluid, etc.)

Positive streamer plasma (sprite), h=60 km

- $v_s = 10^6 \ldots 10^8 \frac{m}{s} \sim c$ (front velocity)
- $n_n = 1{,}5 \times 10^{22} m^{-3}$ (air density)
- $n_e = n_+ = 3 \times 10^{13} m^{-3}$ (NO+, electrons density)
- $\nu_{in} = 6{,}25 \times 10^6 s^{-1}$
- $\nu_{en}(v) \approx 7{,}35 \times 10^8 \ldots 4.29 \times 10^9 s^{-1}$(Itikawa, 2006)
- $T_e = 1{,}25 \times 10^4 K; v_{th,e} = 615 \frac{km}{s}$
- $T_i = 3{,}83 \times 10^3 K; v_{th,i} = 1{,}5 \frac{km}{s}$
- $E_{front} = 66\ kV/m$
- $E_{inside} = 0 \ldots 100 \frac{V}{m}$
- $u_{inside} = 10^5 \frac{m}{s}$ (electrons velocity inside streamer)

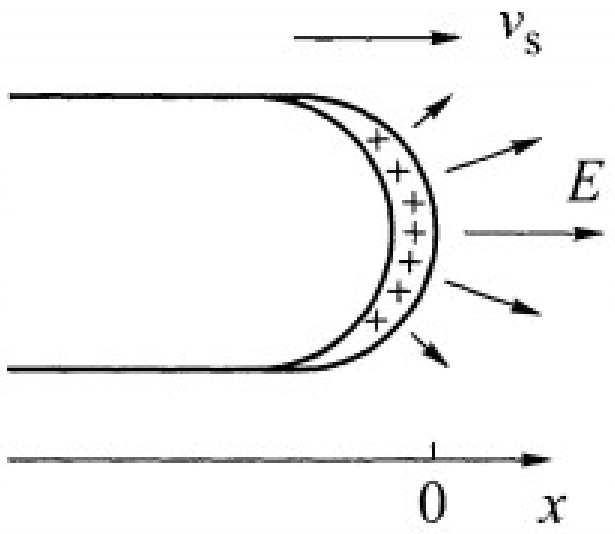

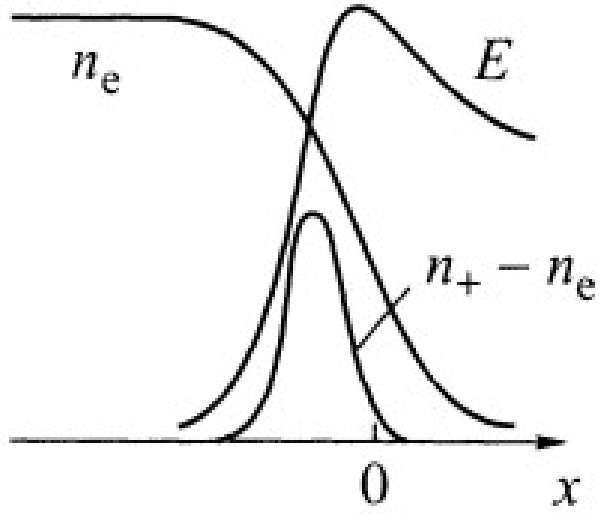

Bazelyan & Raizer, 1998

Scaling laws

- Assuming uniform air composition and constant temperature
- Density falls exponentially with altitude (as the density)

$$p = nk_BT$$

- This influences mean free path, etc.

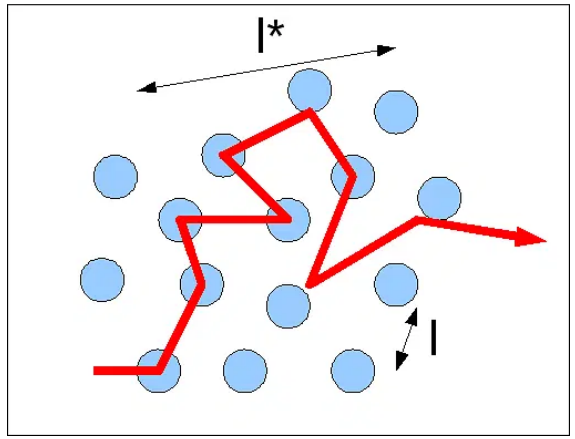

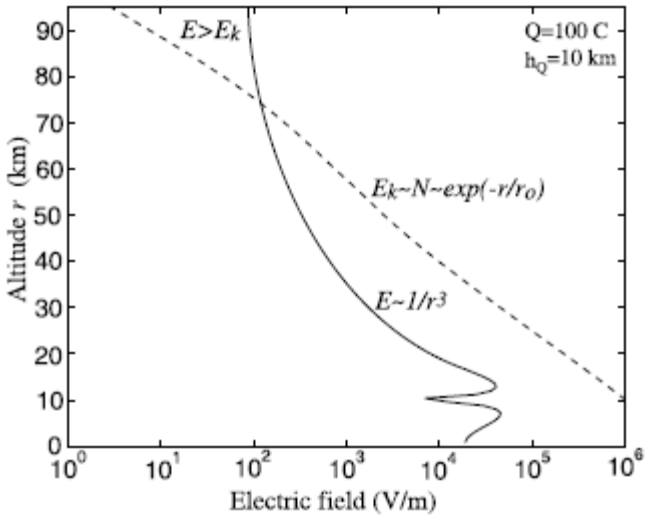

Pasko, 2010

Lengths:
$L \sim n^{-1}$
Times:
$\tau \sim n^{-1}$
Velocities:
$v \sim 1$ (are constant)
Electric fields:
$E \sim n$
Charge densities:
$n_e, n_i \sim n^2$
Relative charge densities (charged particles to neutrals):
$n_e/n \sim n$
Ionization, attachment rates, etc:
$\nu = \frac{1}{\tau} \sim n$
Conductivities:
$\sigma \sim n$
Mobilities:
$\mu \sim n^{-1}$
Current densities:
$j \sim n^2$
Total streamer's current:
$I \sim 1$ (is constant)

Hypotheses of streamer's branching

- Laplace instability (Ebert et al., 1996, Meulenbroek et al., 2004)
- Kinetic diffusive filamentation instability (DFI, Błęcki & Mizerski, 2018)
- Weibel instability (*current filamentation instability, CFI,* Weibel, 1959, Fried, 1959)

Kinetic plasma theory

Describes the evolution of particles' velocity distribution function (i.e. the probability that there are *n* particles around a given velocity $\vec{v}$ and around a given point $\vec{r}$):

$$\frac{\partial f_\alpha}{\partial t} + \vec{v} \cdot \nabla_{\vec{r}} f_\alpha + \frac{q_\alpha}{m_\alpha}(\vec{E} + \vec{v} \times \vec{B}) \cdot \nabla_{\vec{v}} f_\alpha = \left(\frac{\partial f_\alpha}{\partial t}\right)_{coll}$$

Discrete formulation, Klimontovich-Dupree:

$$F(\vec{r}, \vec{v}, t) = \sum_i \delta(\vec{r} - \vec{r}_i(t))\delta(\vec{v} - \vec{v}_i(t)),$$

Maxwellian:

$$\Phi(\vec{v}, t)_\alpha = \left(\frac{m_\alpha}{2\pi k_B T_\alpha}\right)^{3/2} \exp\left(-\frac{m_\alpha v^2}{2k_b T_\alpha}\right)$$

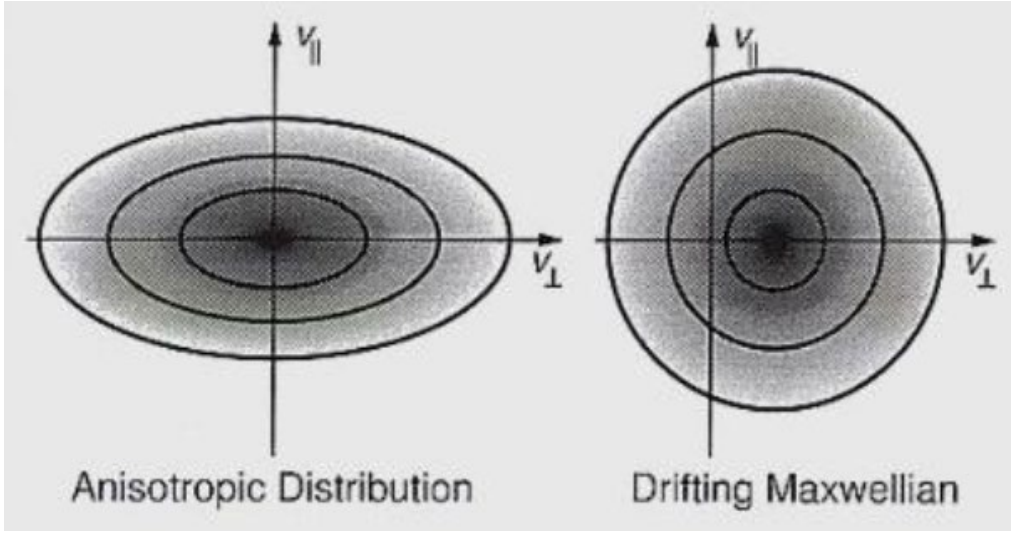

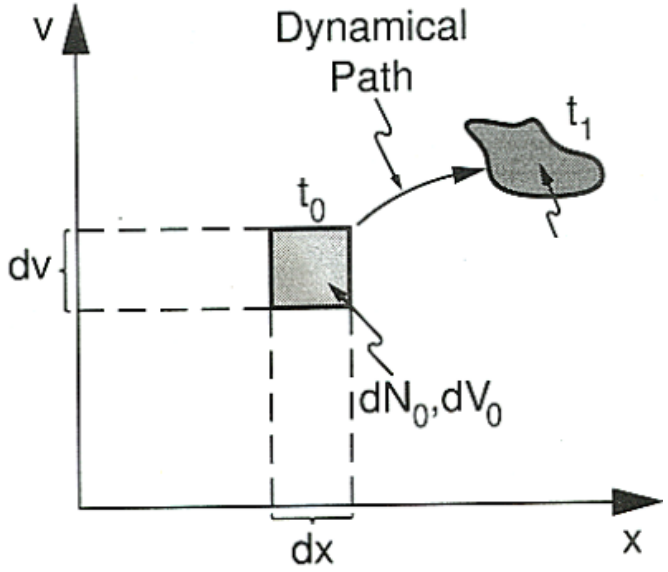

Baumjohann & Treumann, 1997

The first solver (Fourier Boltzmann Solver)

- Solving for Maxwell-Boltzmann system by a spectral method
- Parallel computing (OpenMPI, FFTW-MPI, PLGRID)
- 2D+2V, periodic boundary conditions (implicit in the spectral method)
- BGK collision term
- 2 types of particles: ions, electrons
- Trapezoidal integration
- 3rd order Adams-Bashforth method for derivations of fields and distribution functions:

$$f_\alpha^{t+1} = f_\alpha^t + \Delta t\left(\frac{23}{12}\frac{\partial f_\alpha^t}{\partial t} - \frac{4}{3}\frac{\partial f_\alpha^{t-1}}{\partial t} + \frac{5}{12}\frac{\partial f_\alpha^{t-2}}{\partial t}\right)$$

Fourier Boltzmann Solver

Algorithm 2 Algorithm of the kinetic Boltzmann's equations solver — main loop

1. Calculate densities n_e, n_i, bulk velocities $\langle \vec{v_e} \rangle, \langle \vec{v_i} \rangle$, collisions frequencies ν_e, ν_i for electrons and ions from the moments of their distribution functions.
2. Calculate the current $\vec{j}$.
3. Calculate DFT-densities $\widetilde{n}_e, \widetilde{n}_i$, current $\widetilde{\vec{j}}$ and charge density $\widetilde{\rho}$.
4. Calculate DFT-potential $\widetilde{\varphi}$.
5. Calculate electric field $\widetilde{\vec{E}'} = \widetilde{\vec{E}'}^{t-1} + \partial\widetilde{\vec{E}'}$ and magnetic field $\widetilde{\vec{B}'} = i\vec{k} \times \widetilde{\vec{A}}$.
6. Calculate fields for the next time-step $\widetilde{\vec{E}'}^{t+1} = \widetilde{\vec{E}'} + \partial\widetilde{\vec{E}'}$, $\widetilde{\vec{A}}^{t+1} = \widetilde{\vec{A}} + \partial\widetilde{\vec{A}}$
7. Inverse DFT to get fields $\vec{E}' = \mathcal{F}^{-1}\left[\widetilde{\vec{E}'}\right]$, $\vec{B}' = \mathcal{F}^{-1}\left[\widetilde{\vec{B}'}\right]$.
8. Solve Boltzmann's equations in DFT domain to get the time-derivative $\frac{\partial \widetilde{f_\alpha}}{\partial t}$.
9. Calculate the next time-step distributions $\widetilde{f_\alpha}^{t+1} = \widetilde{f_\alpha} + \Delta t \frac{\partial \widetilde{f_\alpha}}{\partial t}$.
10. Transform the distribution function to basic domain ${f_\alpha}^{t+1} = \mathcal{F}^{-1}[\widetilde{f}_\alpha^{t+1}]$.

$$\nabla \cdot \vec{A} = 0, \tag{7.0.1}$$

$$\nabla^2 \varphi = -\frac{\varrho}{\varepsilon_0}, \tag{7.0.2}$$

$$\vec{B}' = \nabla \times \vec{A}, \tag{7.0.3}$$

$$\vec{E}' = -\nabla\varphi - \frac{\partial \vec{A}}{\partial t}, \tag{7.0.4}$$

$$\frac{\partial \vec{E}'}{\partial t} = \frac{-\nabla^2 \vec{A}}{\mu_0 \varepsilon_0} - \frac{\vec{j}}{\varepsilon_0}, \tag{7.0.5}$$

$$\vec{j} = -en_e\langle \vec{v}_e \rangle + en_i\langle \vec{v}_i \rangle = -e\Gamma_e + e\Gamma_i = -e\int_V \vec{v} f_e d^2v + e\int_V \vec{v} f_i d^2v, \tag{7.0.6}$$

$$\varrho = -en_e + en_i, \tag{7.0.7}$$

$$\frac{\partial f_\alpha}{\partial t} + \vec{v} \cdot \nabla_{\vec{r}} f_\alpha + \frac{q_\alpha}{m_\alpha}(\vec{E}_0 + \vec{E}' + \vec{v} \times \vec{B}') \cdot \nabla_{\vec{v}} f_\alpha = -\nu_\alpha (f_\alpha - n_\alpha \Phi_\alpha), \tag{7.0.8}$$

where e is the elementary charge, φ is the scalar potential, $\vec{A}$ is the vector potential and $\Phi_\alpha = \frac{m_\alpha}{2\pi k_B T_\alpha} \exp\left(-\frac{m_\alpha}{2k_B T_\alpha}(\vec{v}_\alpha - \langle \vec{v}_\alpha \rangle)^2\right)$ is the two-dimensional Maxwellian (note its difference from the 3D case; for the case of $m_e \ll m_i$, $T_{\alpha n} = T_\alpha$ as given above) and n_α and $\langle \vec{v}_\alpha \rangle$ are calculated from velocity moments (Equations 3.1.2, 3.1.3).

Fourier Boltzmann Solver

- Charge conservation
- Simulating Weibel instability
- DFI could not be simulated
- ~3000 lines of the code in C
- Moving to another approach (Particle-in-cell code SMILEI)

SMILEI (Particle in Cell)

- Parallel PIC model (Derouillat et al., 2018), macro-particles of given shape (*S*) and weight (*w*) represent the behavior of much more real particles:

$$F_\alpha(\vec{r},\vec{v},t) = \sum_{i=1}^{N_\alpha} \frac{w_i}{V_c} S(\vec{r}-\vec{r}_i(t))\delta(\vec{v}-\vec{v}_i(t))$$

- Implementing of electron-neutral, ion-neutral collision model: Monte Carlo Collisions (MCC, Vahedi & Surendra, 1995)

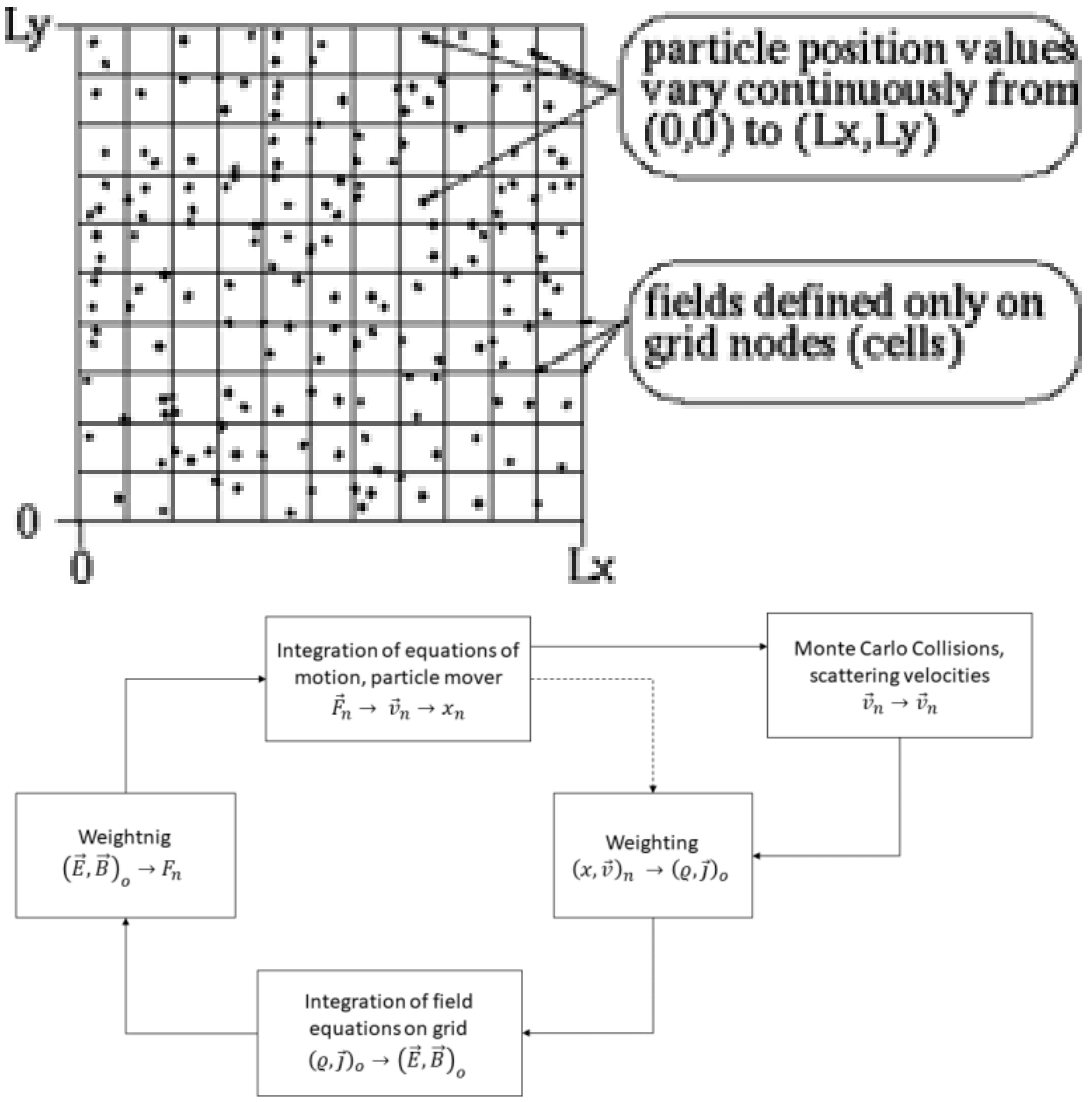

Validation

- Maxwellianization of the distribution
- Investigating collisions of single and multiple particles

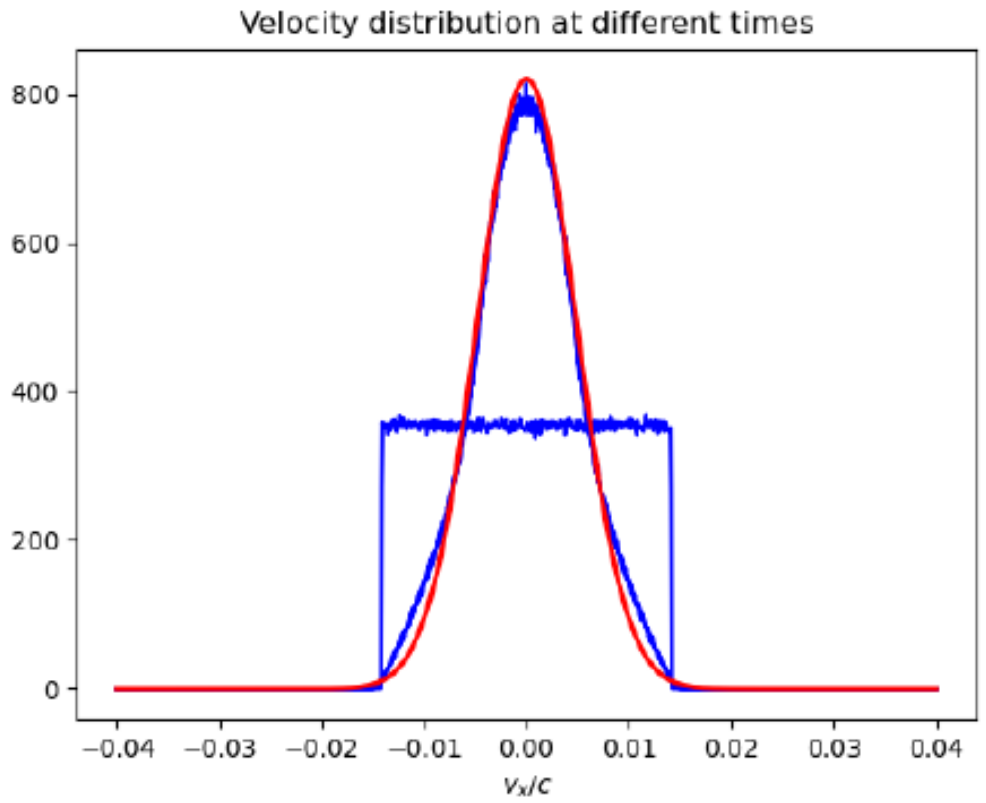

Figure 7: Evolution of electrons' distribution function in v_x direction at different time-steps. The initially rectangular distribution evolves into a Maxwellian-like one. The red line shows a Gaussian function. The density scale for the y-axis is $n_{eScale} = \varepsilon_0 m_e \omega_r^2 = 1.12 \times 10^{27}$ m^{-3}.

Validation

The algorithm was validated on weakly-ionized plasma with various settings. Validation scripts were adapted from SMILEI's benchmark scripts. Purely virtual and immobile neutral particles were involved only in collisions and the collision rate was constant (regardless of the energy of the impeding particle).

The colliding electrons were tested the plasma conductivity behavior. The plasma conductivity can be calculated from the fluid equation of motion:

$$m_\alpha \frac{d\vec{v}_\alpha}{dt} = q_\alpha(\vec{E} + \vec{v}_\alpha \times \vec{B}) - m_\alpha \nu_\alpha(\vec{v}_\alpha - \langle \vec{v}_\alpha \rangle). \tag{12}$$

in the absence of the magnetic field and considering a steady state ($\frac{d\vec{v}}{dt}$) and only electrons to be mobile, we restrict only to the influence of electrons and get:

$$\vec{E} = -\frac{m_e \nu_e}{e} \langle \vec{v}_e \rangle, \tag{13}$$

where e is the elementary charge. The current is given by

$$\vec{j} = -e n_e \langle \vec{v}_e \rangle, \tag{14}$$

which in combination with Equation 13 yields the Ohm's law:

$$\vec{E} = \sigma \vec{j} = \frac{n_e e^2}{m_e \nu_e} \vec{j}, \tag{15}$$

where

$$\sigma = \frac{n_e e^2}{m_e \nu_e} \tag{16}$$

is the plasma conductivity.

At the same time one can derive the steady-state bulk velocity from Equations 14 and 15:

$$\langle \vec{v}_e \rangle = -\frac{\vec{E} e}{m_e \nu_e}. \tag{17}$$

For sprite-like conditions, where $n_e \approx 3.01 \times 10^{13}$ m^{-3}, $\nu_e \approx 2.32 \times 10^9$ s^{-1}, from Equation 16 the conductivity is $\sigma \approx 3.64 \times 10^{-4}$ S m^{-1}. In Figure 6 the simulated evolution of the bulk velocity of electrons is shown for various values of the electric field in dimensionless units. The 1D simulation with reference frequency $\omega_r = 3.09 \times 10^8$ s^{-1} consisted of electrons only, 400 particles per cell, simulation's spatial length $40 \times 2\pi c/\omega_r$, cell length $40 \times 2\pi c/\omega_r$, duration $0.5 \times 2\pi/\omega_r$, time-step $0.001 \times 2\pi/\omega_r$, periodic boundary conditions. One can see that modelled values converge to theoretical ones, however at high fields the velocity overshoots the expectation.

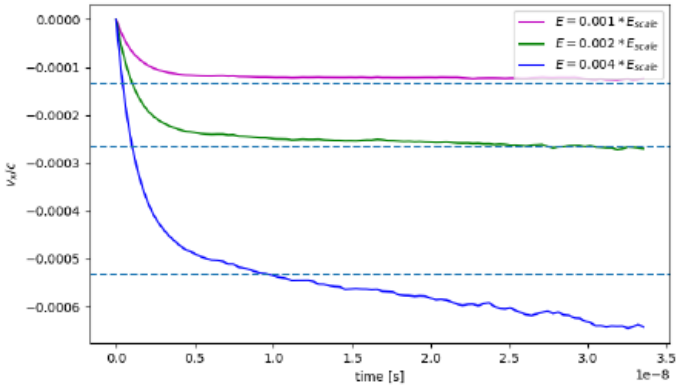

Figure 6: Evolution of the electrons' velocity in sprite streamer conditions at applied constant electric field: $E = 0.001 \times E_{scale} = 5.27 \times 10^2$ V m^{-1} (magenta), $E = 0.002 \times E_{scale} = 1.05 \times 10^3$ V m^{-1} (green) and $E = 0.004 \times E_{scale} = 2.11 \times 10^3$ V m^{-1} (blue). Dashed lines are theoretically predicted bulk velocities at the steady state (Equation 17). $E_{scale} = 5.27 \times 10^5$ V m^{-1}.

DFI (Błęcki & Mizerski, 2018)

- Basing on investigating linearized kinetic equations for small disturbance in a form

$$\sim exp(i(kx - \omega t))$$

- Initial distribution for ions and electrons: drifting Maxwellian
- Dielectric tensor investigation in a moving system (via Lorentz transform) and collisions via BGK (Alexandrov et al., 1984):

$$\left(\frac{\partial f_\alpha}{\partial t}\right)_{coll}^{\alpha\beta} = -\nu_{\alpha\beta}(f_\alpha - n_\alpha \Phi_{\alpha\beta})$$

- $\vec{E} \perp \vec{k}, \vec{k} \perp \vec{u}_e$
- $\omega = i\,\nu_{in}\left(\frac{v_{Thi}\nu_{en}}{v_{The}\nu_{in}} - 1\right) + \delta\omega(k) \sim \nu_{in}, < v >_e, k$, ca. $0{,}4\,\nu_{in} \approx 10^6 s^{-1}$
- Should occur in TLE streamer, $\tau_{DFI} \approx 10^{-6} s$, while $\tau_{TLE} \approx 10^{-2} \ldots 10^{-1} s$

DFI in external electric field at variable collisions rates ν_{en}

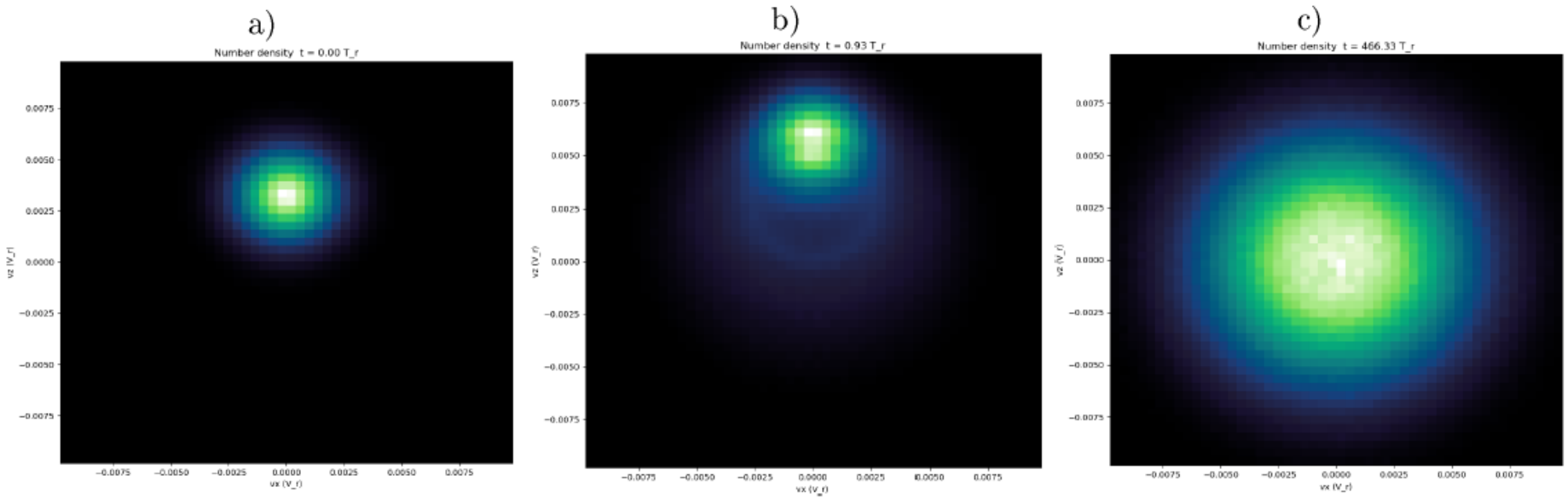

Figure 5.2.4: Evolution of the electron number density distribution in velocity space, plane v_x, v_z. The color code indicates the density with the brightest pixel (white) being currently maximum density (at a given time-step) . Velocity space restricted to $\langle -0.01, 0.01 \rangle c$, DFI, $S_{coll} = 0.1$, $k = 0.2$ m^{-1}.

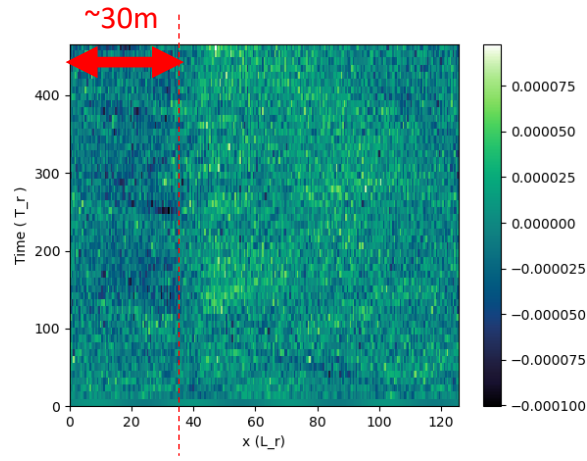

- Disturbance wavelength: 4-63 m (wavenumber $k = [0{,}1; 0{,}2; 0{,}4; 0{,}8; 1{,}6] m^{-1}$), electrons drift $< v >_e$= [100,1000] km/s, external field E_0=[−200 V/m; −66 kV/m], $S_{coll}[10^{-3} \ldots 10^{1}]$)
- Fast set-on of nonlinear effects, strong suppressing influence of collisions ($\nu_{en} \approx 1{,}3 \times 10^9 s^{-1} \times S_{coll}$) which introduce the noise in charge density and B field patterns
- Fast relaxation (Maxwellianization) of the distribution due to collisions
- Only for $\nu_{en} \approx 1{,}3 \times 10^9\ s^{-1}$ ($S_{coll} = 1$), some DFI-like pattern is visible, $\lambda \approx 31m, k = 0{,}2m^{-1}$, $\mathrm{T}_r = \omega_{pe} \approx 3 \times 10^8 s^{-1}$, $\mathrm{L}_r \approx 1m$

DFI-like, no external electric field

- Some exponential growth, rate $1{,}66 \times 10^4 s^{-1}$ (DFI growth: $\sim 10^6 s^{-1}$)
- Could be investigated with linearized equations, but it is not the DFI

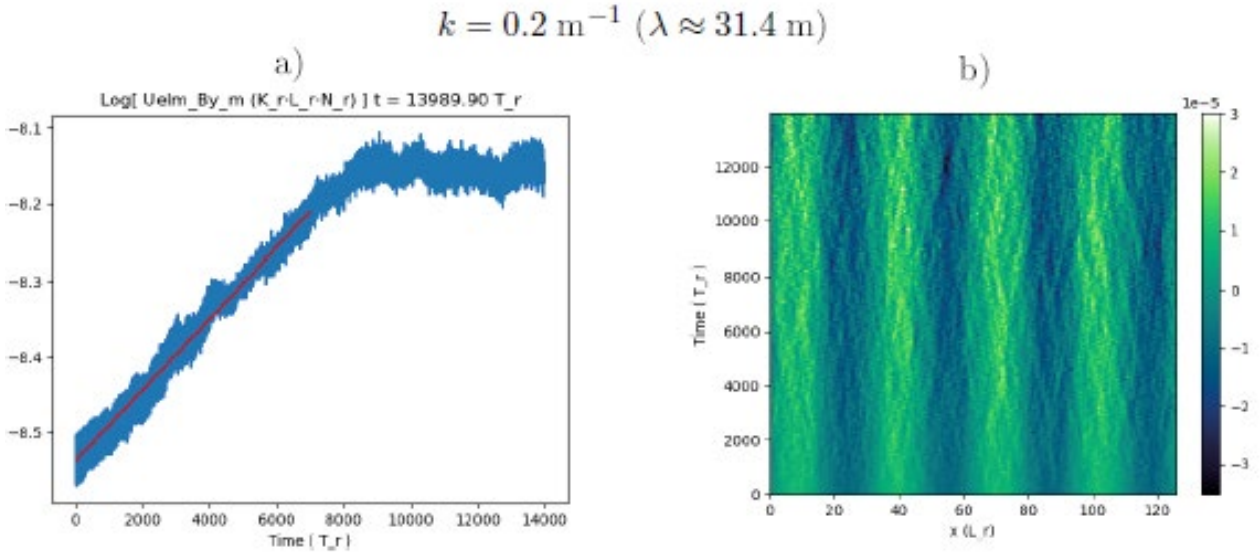

Figure 5: Logarithm of the magnetic energy density $U_{elm,By}$ vs time (a) and magnetic field evolution vs time (b); case without external electric field, $k = 0.2\ \mathrm{m}^{-1}$, $S_{coll} = 10^{-5}$ (red line is the exponential fit).

Weibel instability (CFI) at variable collisions rates ν_{en}

- No in-situ measurements of streamer channels
- Assumption of 2 counter-streaming streams of particles (for the appearance of a counter-stream in plasma when single stream is injected, e.g. Cox, 1970)
- No external electric field inside streamer
- Cold distributions (v_{The} , $v_{Thi} = 0$)
- CFI growth rate investigation at different modes and collisions rates ($\times S_{coll}[10^{-9} \ldots 10^{-3}]$)

CFI, evolution of electron's distribution (v_x, v_z plane)

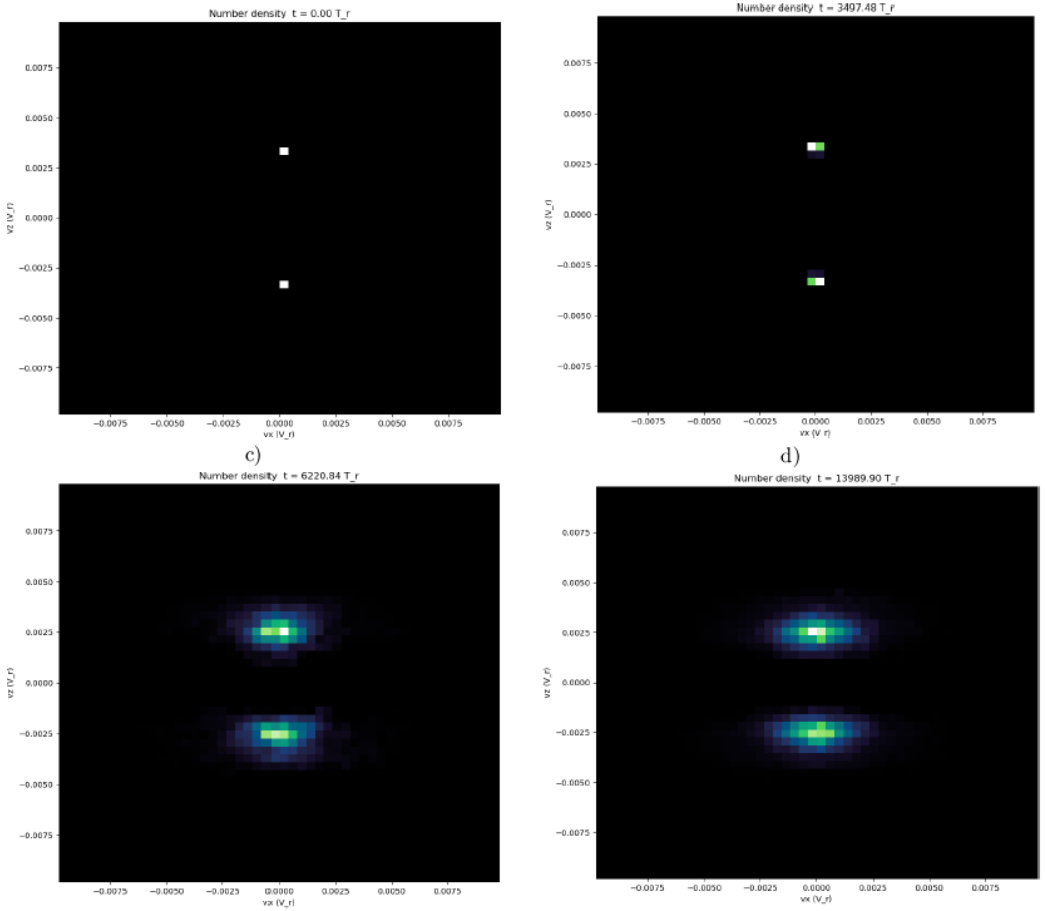

$S_{coll} = 10^{-7}$ (as in FBS)

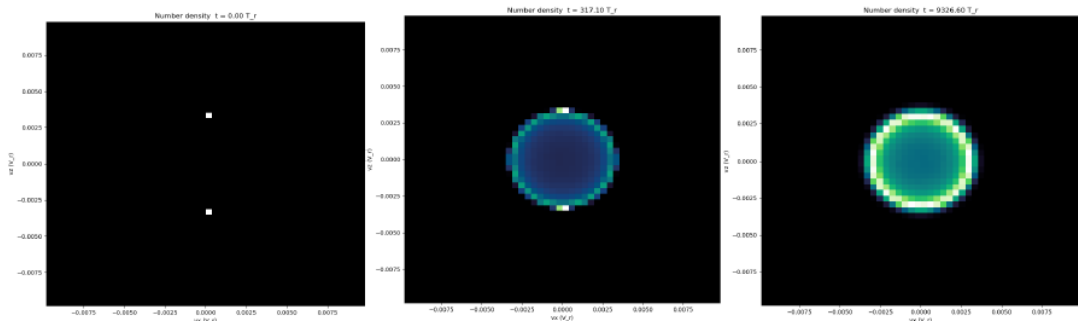

$S_{coll} = 10^{-3}$

CFI

- B_y in time and space, 1D (nonlinear effect of collisions, $S_{coll} = 10^{-5}$, $\nu_{en} \approx 1{,}3 \times 10^4\ s^{-1}$),

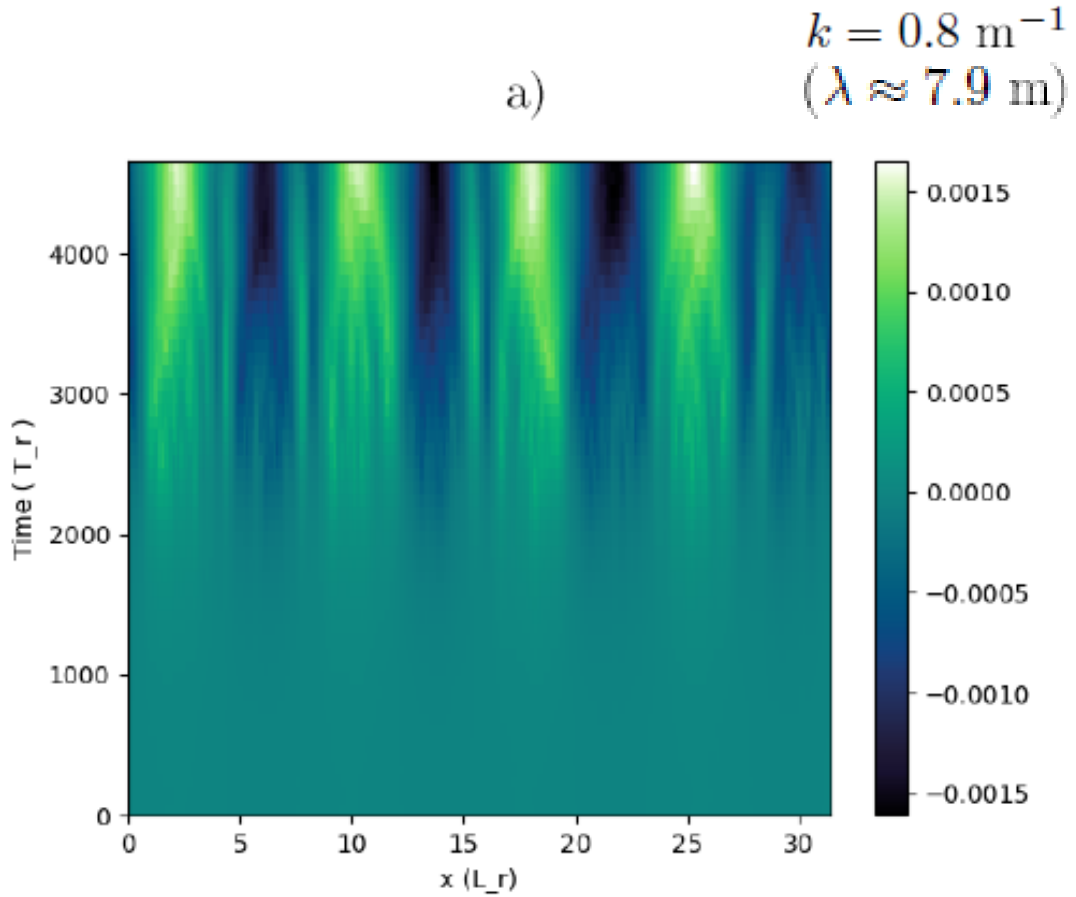

CFI, magnetic field energy growth rate

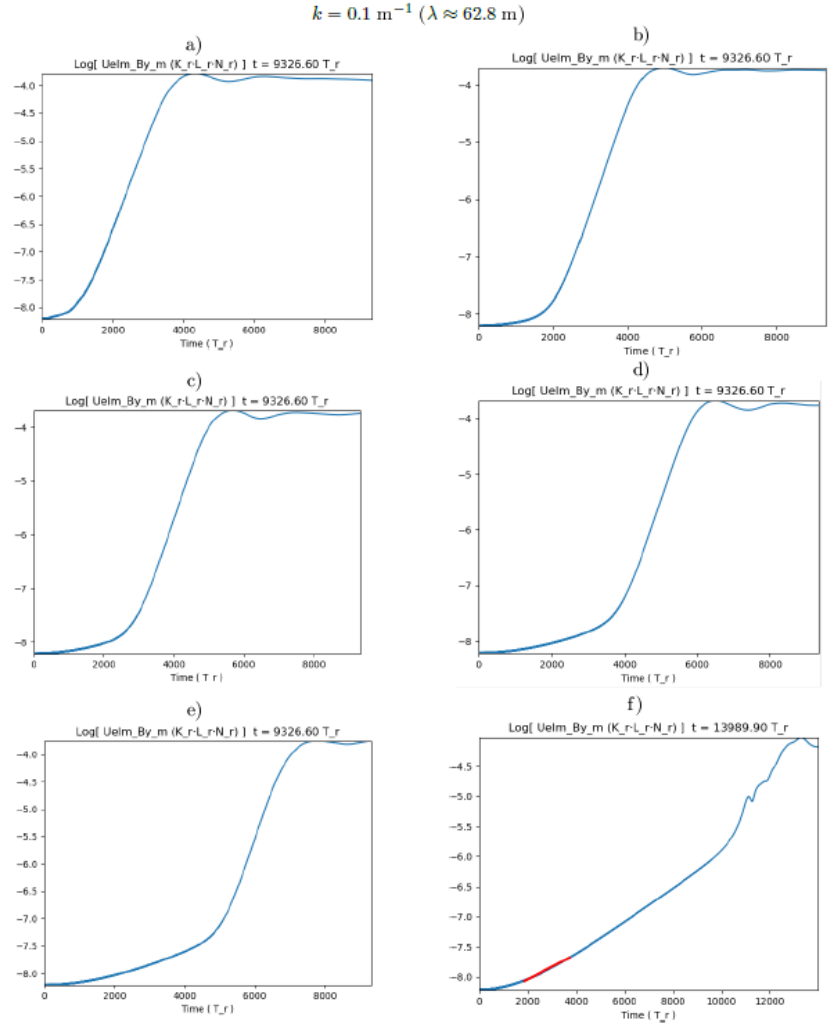

Figure 5.3.8: Logarithm of the magnetic energy density $U_{elm,By}$ vs time; the CFI, $k = 0.1\ \mathrm{m}^{-1}$, a) $S_{coll} = 10^{-5}$, b) $S_{coll} = 10^{-6}$, c) $S_{coll} = 10^{-7}$, d) $S_{coll} = 10^{-8}$, e) $S_{coll} = 10^{-9}$, f) without collisions (red line is fitted for Fourier-isolated growth rate).

- *Fourier isolated growth rate* for single wavelength
- Secondary instability of exponential growth rate (depending on collisions rate)
- Suppressing CFI at different collisions rates ($\nu_{en} \approx 1{,}3 \times 10^9 s^{-1} \cdot S_{coll}$), drastically when the MFP (*mean free path*) gets close to the disturbance wavelength

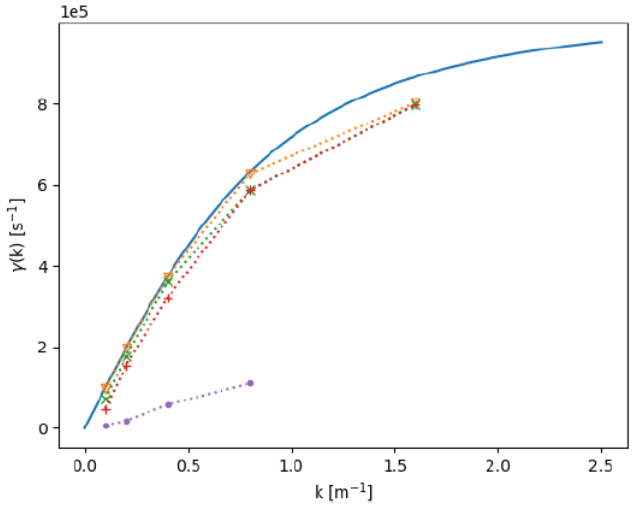

Figure 5.3.3: Growth rates of the CFI. Solid blue line indicates theoretical values, yellow triangles ('∇') correspond to collisionless simulation, green x's ('×') to $S_{coll} = 10^{-6}$, red pluses ('+') to $S_{coll} = 10^{-5}$, purple points ('•') to $S_{coll} = 10^{-4}$.

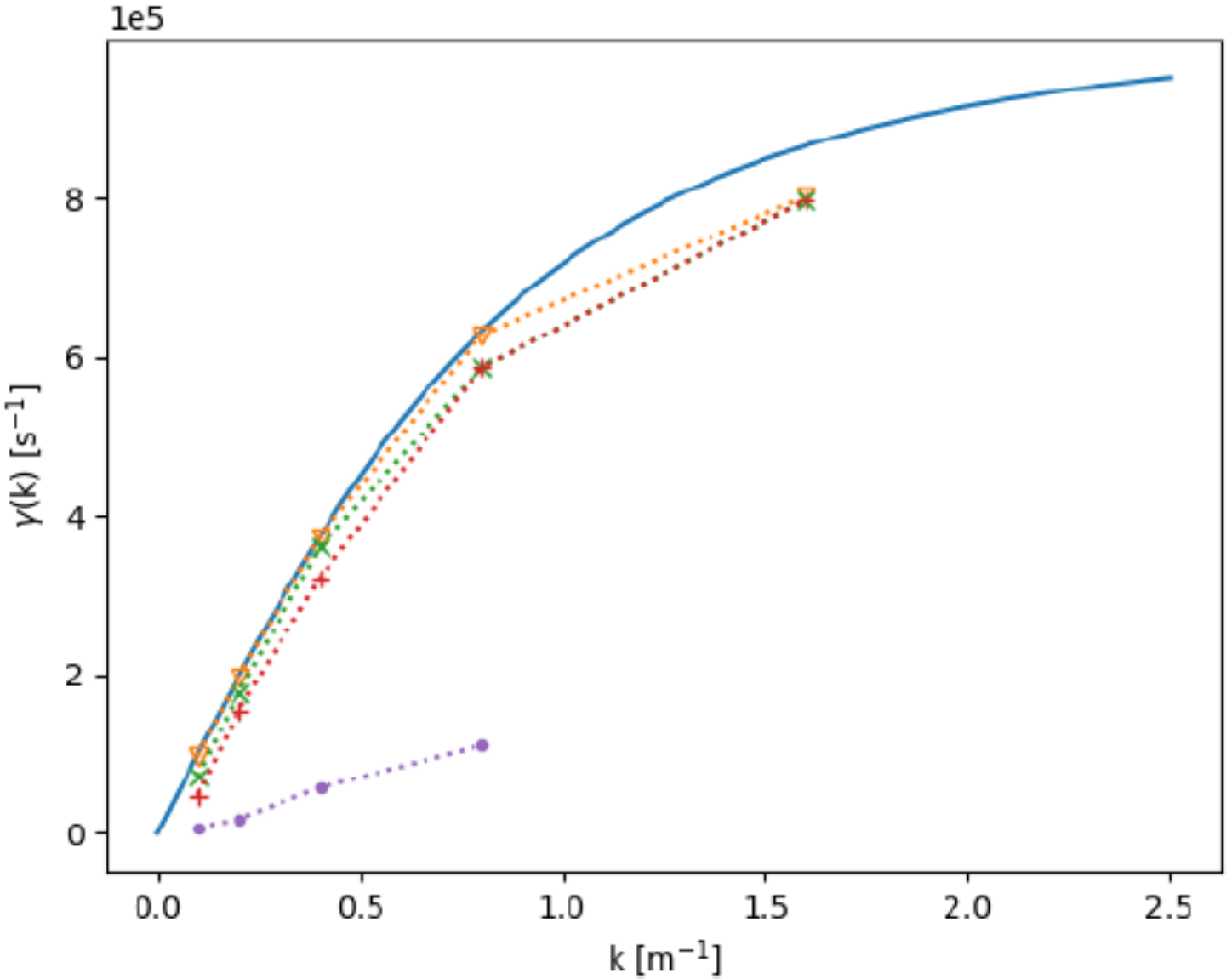

Figure 5.3.3: Growth rates of the CFI. Solid blue line indicates theoretical values, yellow triangles ('∇') correspond to collisionless simulation, green x's ('$\times$') to $S_{coll} = 10^{-6}$, red pluses ('+') to $S_{coll} = 10^{-5}$, purple points ('$\bullet$') to $S_{coll} = 10^{-4}$.

Conclusions

- PIC+MCC code with analysis methods were given
- Strong suppression of instabilities due to collisions
- Fast on-set of nonlinear effects
- DFI: some patter visible in one case, fast Maxwellianization of the distribution, breaks the foretaken theoretical assumption, discrepancy between the drift velocity and the external electric field made BGK model not working
- some linear instability visible when no external electric field was given
- CFI: the biggest suppression when $MFP \sim \lambda$, secondary instability due to collisions
- FBS to be developed in the future
- Plans:
  - 2 publications: CFI, DFI
  - Further analysis of the DFI, simulating conditions when the DFI sets on (non-TLE)
  - Improvement and simulations: SMILEI+MCC i FBS
  - Investigation of Laplace instability with the kinetic theory and with collisions

Laplacian instability, Lozansky-Firsov limit

$$\nabla^2\varphi(x,y)=0 \quad \text{(outside the streamer)}, \qquad (1)$$

$$-\nabla\varphi(x,y)\to E_0\hat{x} \quad \text{(far outside the streamer)}, \qquad (2)$$

$$\varphi(x,y)=0 \quad \text{(inside the streamer)}, \qquad (3)$$

$$v_{\text{bound}}=c\,\nabla\varphi_{\text{bound}} \quad \text{(velocity of the boundary)}, \qquad (4)$$

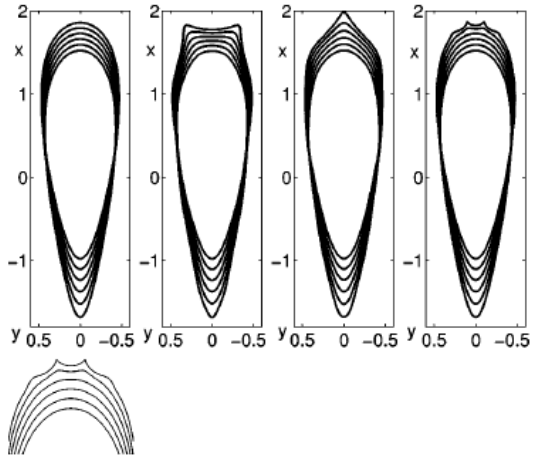

FIG. 1. Upper panel: evolution of the interface in equal time steps up to time $t=0.1/(E_0c)$ with initial condition (a) $z_0(\alpha,0)=e^{-i\alpha}+0.6e^{i\alpha}-0.08e^{2i\alpha}$, (b) $z(\alpha,0)=z_0(\alpha,0)-5\times10^{-3}e^{8i\alpha}$, (c) $z(\alpha,0)=z_0(\alpha,0)+3\times10^{-3}e^{8i\alpha}$, and (d) $z(\alpha,0)=z_0(\alpha,0)-4.5\times10^{-7}e^{30i\alpha}$. Lower panel: zoom into the unstable head of panel (d).

Meulenbroek, 2004

- Calculating for a potential of a conducting ellipsoid in 2d (Landau & Lifshitz)
- No charge outside the streamer
- Ideal conductivity inside
- System prone to an instability on a harmonic mode
- Firstly published by Lozansky & Firsov (1973)
- Similar moving boundary problems arise in Hele-Shaw flow of two fluids with a large viscosity contrast

Bibliography

- Alexandrov, Andrey F., Larisa S. Bogdankevich, & Anri A. Rukhadze. Principles of Plasma Electrodynamics. Berlin, Heidelberg: Springer Berlin Heidelberg, 1984. https://doi.org/10.1007/978-3-642-69247-5.
- Baumjohann, Wolfganf, & Rudolf A. Treumann. *Basic Space Plasma Physics*. Reprinted. London: Imperial College Press, 2006.
- Bazelyan, E. M., & Yuri P. Raizer. *Spark Discharge*. Boca Raton, Fla: CRC Press, 1998.
- Błęcki, Jan, & Krzysztof Mizerski. „Subtle structure of streamers under conditions resembling those of Transient Luminous Events". Archives of Mechanics 70, nr 6 (2018): 1–16. https://doi.org/10.24423/aom.3009.
- Ebert, Ute, Wim van Saarloos, & Christiane Caroli. „Streamer Propagation as a Pattern Formation Problem: Planar Fronts". Physical Review Letters 77, nr 20 (11 listopad 1996): 4178–81. https://doi.org/10.1103/PhysRevLett.77.4178.
- Fasoulas, S., C.-D. Munz, M. Pfeiffer, J. Beyer, T. Binder, S. Copplestone, A. Mirza, P. Nizenkov, P. Ortwein, & W. Reschke. „Combining Particle-in-Cell and Direct Simulation Monte Carlo for the Simulation of Reactive Plasma Flows". Physics of Fluids 31, nr 7 (1 lipiec 2019): 072006. https://doi.org/10.1063/1.5097638.
- Franz, R. C., R. J. Nemzek, & J. R. Winckler. „Television image of a large upward electrical discharge above a thunderstorm system". Science, 1990. https://doi.org/10.1126/science.249.4964.48.
- Fried, Burton D. „Mechanism for Instability of Transverse Plasma Waves". Physics of Fluids 2, nr 3 (1959): 337. https://doi.org/10.1063/1.1705933.
- Gerken, Elizabeth A., Umran S. Inan, & C. P. Barrington-Leigh. „Telescopic imaging of sprites". Geophysical Research Letters 27, nr 17 (2000): 2637–40. https://doi.org/10.1029/2000GL000035.
- Itikawa, Yukikazu. „Cross Sections for Electron Collisions with Nitrogen Molecules". Journal of Physical and Chemical Reference Data 35, nr 1 (marzec 2006): 31–53. https://doi.org/10.1063/1.1937426.
- Meulenbroek, Bernard, Andrea Rocco, & Ute Ebert. „Streamer Branching Rationalized by Conformal Mapping Techniques". Physical Review E 69, nr 6 (17 czerwiec 2004): 067402. https://doi.org/10.1103/PhysRevE.69.067402.
- Okhrimovskyy, A., A. Bogaerts, & R. Gijbels. „Electron Anisotropic Scattering in Gases: A Formula for Monte Carlo Simulations". Physical Review E 65, nr 3 (27 luty 2002): 037402. https://doi.org/10.1103/PhysRevE.65.037402.
- Surkov, V. V., & Masashi Hayakawa. „Underlying mechanisms of transient luminous events: A review". Annales Geophysicae 30, nr 8 (2012): 1185–1212. https://doi.org/10.5194/angeo-30-1185-2012.
- Teunissen, Jannis, & Ute Ebert. „3D PIC-MCC Simulations of Discharge Inception around a Sharp Anode in Nitrogen/Oxygen Mixtures". Plasma Sources Science and Technology 25, nr 4 (1 sierpień 2016): 044005. https://doi.org/10.1088/0963-0252/25/4/044005.
- Vahedi, V., & M. Surendra. „A Monte Carlo Collision Model for the Particle-in-Cell Method: Applications to Argon and Oxygen Discharges". Computer Physics Communications 87, nr 1–2 (maj 1995): 179–98. https://doi.org/10.1016/0010-4655(94)00171-W.
- Weibel, Erich S. „Spontaneously Growing Transverse Waves in a Plasma Due to an Anisotropic Velocity Distribution". Physical Review Letters 2, nr 3 (1 luty 1959): 83–84. https://doi.org/10.1103/PhysRevLett.2.83.

DFI in external electric field at variable collisions rates ν_{en}

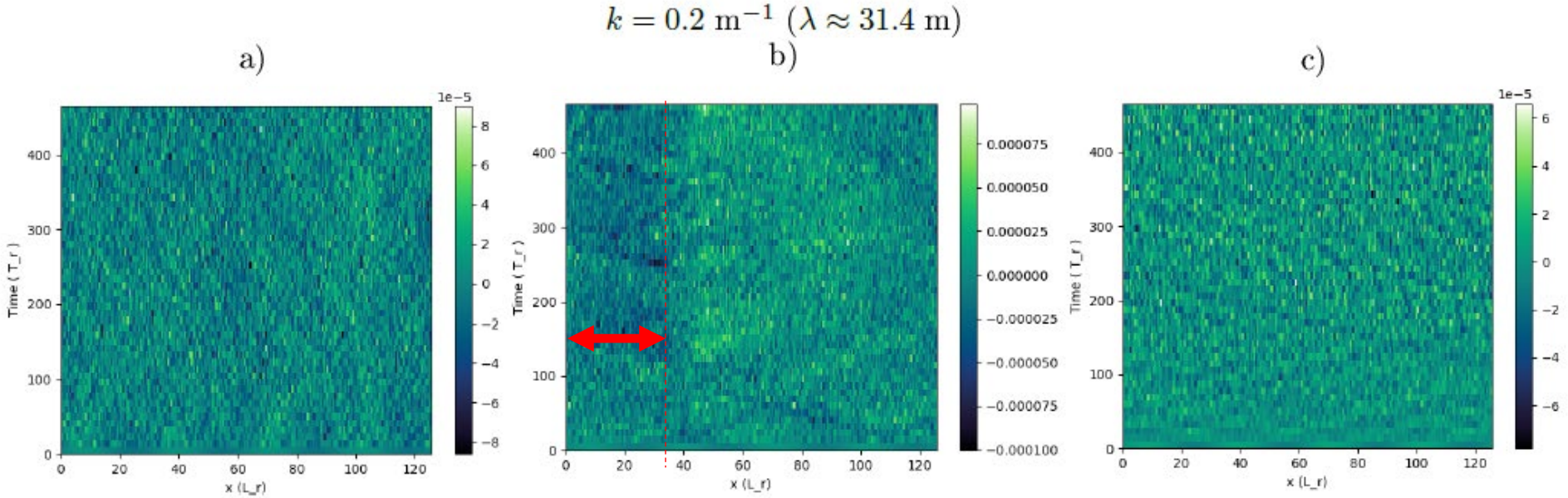

Figure 5.2.1: Magnetic field evolution vs time; DFI, $k = 0.2\,\mathrm{m}^{-1}$, a) $S_{coll} = 0.1$, b) $S_{coll} = 1$, c) $S_{coll} = 10$.